

# Crystallization of gel-derived mullite-zirconia composites

I. M. LOW\*, R. McPHERSON

Department of Materials Engineering, Monash University, Clayton 3168, Victoria, Australia

The crystallization of gel-derived mullites containing  $ZrO_2$  content up to 20 wt% had been studied. The formation of a metastable solid solution between  $ZrO_2$  and mullite was established. A model was proposed to account for the formation of this solid solution. Grain refinement of mullite grains was observed in the composites containing at least 7 wt%  $ZrO_2$ .

## 1. Introduction

Mullite- $ZrO_2$  composites may be prepared by a variety of methods. Claussen and Jahn [1] prepared mullite- $ZrO_2$  composites from the reaction between alumina and zircon and obtained significant improvement in toughness and strengths over pure mullites. This *in situ* reaction produced fine  $ZrO_2$  particles which were uniformly dispersed in the matrix of mullite. However, the ceramic prepared by this process has an essentially constant phase composition and thus precludes optimization of the mechanical behaviour with respect to the  $ZrO_2$  volume fraction, as was advantageous in the  $Al_2O_3$ - $ZrO_2$  system [2]. In view of this, Prochazka *et al.* [3] prepared mullite- $ZrO_2$  composites from fused mullite and up to 25 vol%  $ZrO_2$  may be incorporated. They observed that addition of  $ZrO_2$  promoted densification and retarded grain growth of the mullite phase. Recent developments in the gel technology have enabled these composites to be prepared and fabricated with much ease [4-6]. This technique allows a greater flexibility in the incorporation of metastable  $ZrO_2$  particles into the mullite matrix as compared to the plasma method [7].

None of the above investigators studied or measured the solid solution of zirconia in the matrix of mullite which could have a significant influence on the modification and control of the physical and mechanical properties of these composites in relation to the resultant microstructures and grain sizes, as in metallic alloys. Unlike the latter, the value of solid solution between zirconia and mullite is expected to be small in view of the large ionic radius associated with zirconium ions. This was demonstrated by Moya and Osendi [8, 9] where a value of 0.5 wt%  $ZrO_2$  was obtained for mullite at 1570°C. At 1600°C Pena and Aza [10] found a value of about 0.1 wt%  $ZrO_2$ . The underlying mechanisms of this solid solution remain enigmatic although a simple substitution of zirconium for aluminium ions has been suggested [9].

The objective of this paper was to prepare gel-derived mullite-zirconia composites with the aim of measuring the solid solution of zirconia in mullite at a particular temperature. The microstructure modifi-

cation by the addition of zirconia in relation to the phase transition and grain refinement of mullite was also investigated. An attempt was made to formulate a model concerning the mechanism(s) of metastable solid solution formation between zirconia and (2:1) mullite.

## 2. Experimental procedures

Commercial purity zirconium chloride, silicon tetraethoxide and laboratory prepared aluminium isopropoxide [11] were used as starting raw materials for the preparation of gels. Initially, all the chemicals were mixed in a plastic cup containing some carbon tetrachloride as a common solvent. The mixture was then diluted with dry ethanol and the plastic cup was immersed in chilled water for 0.5 h to enable the *in situ* formation of zirconium tetraethoxide to take place. The resultant solution was then hydrolysed dropwise with water under vigorous stirring. Upon completion of hydrolysis, a plastic film with several holes was used to seal the cup and the solution was allowed to gel over a period of several days in a constant humidity oven in which the temperature was increased in steps from 40 to 80°C. Up to 20 wt% zirconia was incorporated into the mullite (3:2 composition) matrix. It is anticipated that the *in situ* prepared zirconium tetraethoxide would permit a better homogeneity in gels and minimize the premature hydrolysis of the alkoxide.

Differential thermal analysis (DTA) of the gel was performed with a Rigaku Micro DTA apparatus at a heating rate of 10°C min<sup>-1</sup>. A Philips X-ray diffractometer (PW 1050/25 wide-angle goniometer) was used to identify the crystalline phases formed in heat-treated gels. Finely ground gel powder was placed on an aluminium disc as a substrate and a nickel-filtered  $CuK\alpha$  radiation was used. The specimen for transmission electron microscopy (Joel 100c) was prepared by ion-beam thinning.

## 3. Results

### 3.1. Phase relations at various temperatures

Petrographic phase analyses of mullite-zirconia composites are shown in Table I. The results reveal

\* Present address: Department of Materials Engineering, Curtin University of Technology, GPO Box U 1987, Perth, 6001, Australia.

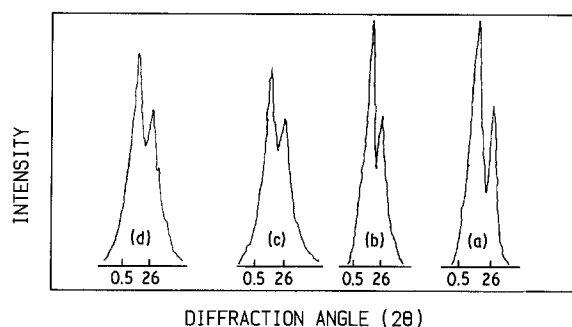


Figure 1 (1 2 0) and (2 1 0) reflections of mullite containing various amount of zirconia heat treated at 1300°C. (a) 0.5 wt % ZrO<sub>2</sub>; (b) 1 wt % ZrO<sub>2</sub>; (c) 2 wt % ZrO<sub>2</sub>; (d) 5 wt % ZrO<sub>2</sub>.

that prior to the formation of mullite phases, an Al-Si spinel was formed. At about 1100°C (depending on zirconia contents), the spinel was observed to coexist with the metastable mullite phase. As in pure mullites [12], the (1 2 0) and (2 1 0) lines of mullites formed here were not distinctly split at this temperature. A rather broad and diffuse peak was obtained. The same feature applies to (2 5 0) and (5 2 0) lines with the latter missing occasionally. The spinel appeared to vanish at or near the onset of the splitting of the (1 2 0) and (2 1 0) lines which occurred at  $\approx 1250^\circ\text{C}$  with the subsequent formation of the orthorhombic mullite. In contrast to pure mullites [12], very small amounts of  $\theta$  and/or  $\alpha$  alumina were always present in the composites treated at 1300°C.

Apparently, the addition of zirconia enhanced the mullitization and the concomitant formation of (3 : 2) mullite (Fig. 1). The splitting of (1 2 0) and (2 1 0) lines occurred at much lower temperatures than in pure mullites. This phenomenon is most clearly depicted in the composites with 0.5 and 1.0 wt % zirconia which formed a solid solution with mullite at temperatures below 1300°C. The results in Table I also indicate that the formation of a solid solution between zirconia and mullite is highly sensitive to temperature and time. The lower the temperature or the shorter the heating time, the higher the solubility limit and vice versa. A

value of 5 wt % was found to be the absolute optimum solubility limit of zirconia in mullite. At that composition, both metastable phases of zirconia and mullite appeared to crystallize out concurrently. For composites with zirconia content greater than 5 wt %, tetragonal zirconia formed prior to the crystallization of (2 : 1) mullite. In short, the metastable form of mullite has a much higher content of zirconia in solid solution than the (3 : 2) mullite.

It is revealed in Table I that there exists a wide range of crystallization temperature,  $T_c$ , for the metastable phase of zirconia in the mullite-zirconia composites, the magnitude of which depended sensitively on the amount of zirconia present. For instance, the  $T_c$  in the composite with 0.5 wt % zirconia was 1400°C while that with 5 wt % was  $\approx 1100^\circ\text{C}$ . It was even lower for higher contents of zirconia [5, 13].

As in pure (3 : 2) mullite [12], mullite-zirconia composites gave a strong exothermic peak (although less sharp) at about 970°C in the DTA curve (Fig 2). A second exotherm at  $\approx 1250^\circ\text{C}$  was observed in all the composites.

From the results obtained (Table I and Fig. 1) and the conclusions reached elsewhere [12] the first exotherm can be identified with the formation of the spinel. Similarly, the second exotherm is attributed to the disappearance of the spinel and the concomitant formation of the (3 : 2) mullite. The endotherms at about 120 and 300 to 500°C were the consequences of dehydration of the gel and dehydroxylation of residual alkoxides, respectively.

### 3.2. Variation of mullite cell dimensions

The cell edge,  $a$ , is plotted against composition of mullite containing zirconia in Fig. 3a. The straight line relationship between cell edge,  $a$ , and cell volume,  $C_v$ , depicted in Fig. 3b lies between the lines of best fit obtained by Cameron [14] and Schneider and Wohlleben [15]. Fig. 3c shows the variation of mullite lattice parameters with the ZrO<sub>2</sub> content. The composition of mullite (mol % Al<sub>2</sub>O<sub>3</sub>) for the composites as a function of temperature is displayed in Fig. 4a.

TABLE I XRD phase analyses of mullite-zirconia composites

Temperature (°C)	Time (h)	Amount of Zirconia (wt %)				
		0.5	1.0	2.0	5.0	$\geq 7.0$
600	0	A	A	A	A	A
1000	0	A	A	A	M <sub>t</sub> , $\gamma_s$	$\gamma_s$ , TZ <sub>w</sub>
1200	0	M <sub>m</sub> , $\gamma_m$	M <sub>m</sub> , $\gamma_s$	M <sub>m</sub> , $\gamma_s$	M <sub>m</sub> , $\gamma_s$ , TZ <sub>w</sub>	M <sub>m</sub> , $\gamma_s$ , TZ <sub>m</sub>
1270	0	M <sub>s</sub> , $\theta_w$	M <sub>s</sub> , $\theta_w$	M <sub>s</sub> , $\gamma_m$ , TZ <sub>t</sub>	M <sub>s</sub> , $\theta_t$ , TZ <sub>m</sub>	M <sub>s</sub> , $\theta_w$ , TZ <sub>m</sub>
1300		M <sub>s</sub> , $\theta_w$	M <sub>s</sub> , $\theta_w$ , TZ <sub>t</sub>	M <sub>s</sub> , $\theta_t$ , TZ <sub>w</sub>	M <sub>s</sub> , $\theta_w$ , TZ <sub>m</sub>	M <sub>s</sub> , $\theta_w$
1300	2	M <sub>s</sub> , $\theta_t$ , TZ <sub>t</sub>	M <sub>s</sub> , $\theta_w$ , TZ <sub>w</sub>	M <sub>s</sub> , $\theta_t$ , TZ <sub>w</sub>	M <sub>s</sub> , $\theta_w$ , TZ <sub>s</sub>	M <sub>s</sub> , $\theta_t$
1300	10	M <sub>s</sub> , $\theta_t$ , TZ <sub>w</sub>	M <sub>s</sub> , $\theta_w$ , TZ <sub>m</sub>	M <sub>s</sub> , $\theta_w$ , TZ <sub>m</sub>	M <sub>s</sub> , $\theta_w$ , TZ <sub>s</sub>	TZ <sub>s</sub> , MZ <sub>m</sub>
1400	0	M <sub>s</sub> , $\theta_t$ , TZ <sub>t</sub>	M <sub>s</sub> , $\theta_w$ , TZ <sub>w</sub>	M <sub>s</sub> , $\theta_w$ , TZ <sub>m</sub>	M <sub>s</sub> , $\theta_w$ , TZ <sub>s</sub>	M <sub>s</sub> , $\alpha_t$
1500	0	M <sub>s</sub> , $\alpha_t$ , TZ <sub>w</sub>	M <sub>s</sub> , $\alpha_t$ , TZ <sub>m</sub>	M <sub>s</sub> , $\alpha_t$ , TZ <sub>m</sub>	M <sub>s</sub> , $\alpha_t$ , TZ <sub>s</sub>	TZ <sub>s</sub> , MZ <sub>s</sub>
						M <sub>s</sub> , $\alpha_t$
						TZ <sub>s</sub> , MZ <sub>s</sub>

A, Amorphous.

$\gamma$ , Al-Si spinel; M, mullite;  $\theta$ ,  $\alpha = \theta$  and  $\alpha$  Al<sub>2</sub>O<sub>3</sub>.

TZ, MZ, tetragonal and monoclinic ZrO<sub>2</sub>, respectively.

s = strong; m = medium; w = weak; t = trace.

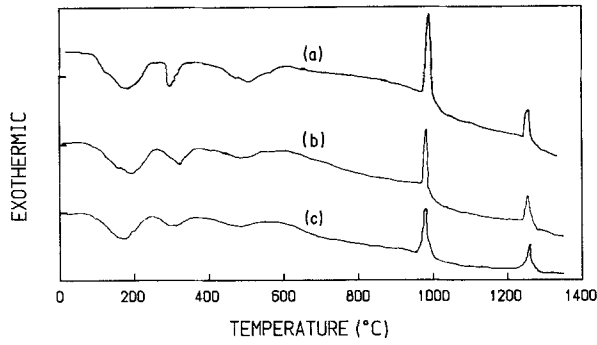
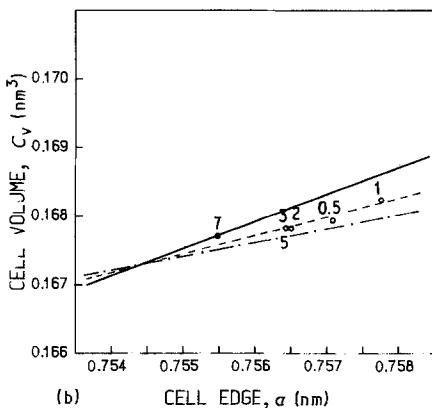
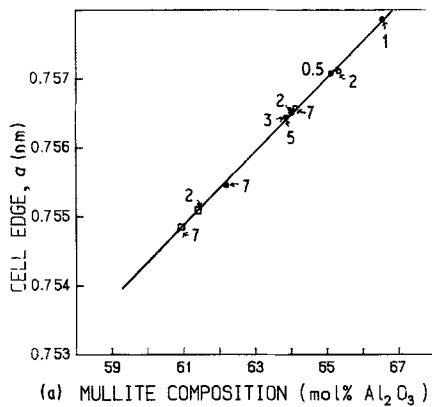


Figure 2 DTA curves of some mullite-zirconia gels. (a) 0.5 wt %  $ZrO_2$ ; (b) 2 wt %  $ZrO_2$ ; (c) 7 wt %  $ZrO_2$ .

The dependence of mullite composition on the time of equilibrium heating at  $1300^\circ C$  is depicted in Fig. 4b. These results indicate that the mullites formed initially approximate to a (2:1) composition and approach a (3:2) composition with increasing temperature and time. The formation of a solid solution between zirconia and mullite is substantiated by the variation of cell dimensions of mullite with the amount of zirconia present.

The extent of solid solution of zirconia in mullite is shown in Fig. 5a. From the graph, the solubility limit of zirconia in mullite is about 0.9 wt % at  $1300^\circ C$ . The sensitivity of this value is revealed in Fig. 5b, where the solubility limit was observed to decrease with increasing temperature and time. This observation is consistent with the results reported in the literature [9, 10] and serves to suggest that the formation of solid solutions between zirconia and mullite at the range of temperatures employed in this work is metastable. The peaks in Fig. 5b correspond to the temperature at which the cell volume of mullite reaches the maximum



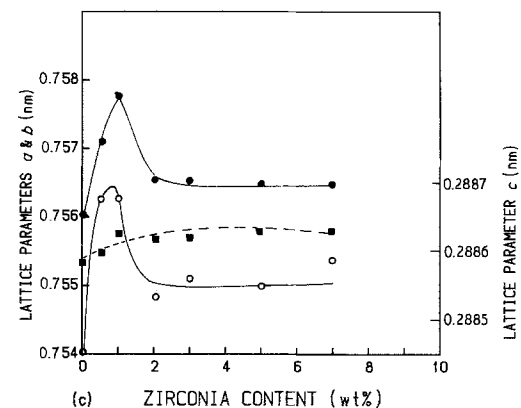
and they serve to represent the metastable solubility limits of zirconia in the composites. With increasing zirconia content, the temperature at which the peak occurs decreases.

### 3.3. Grain size measurement of mullite

X-ray line broadening measurements indicated that grain size of mullite increases rapidly with temperature and grain refinement of mullite could be achieved by the addition of zirconia. The presence of zirconia in solid solution ( $< 1$  wt %) appeared to enhance the grain growth of mullite dramatically (Fig. 6). The grain growth controlling effect of zirconia is clearly depicted in Fig. 7 where only in composites with zirconia contents greater than 5 wt % was there any observable grain refinement of mullite with increasing temperature and time. The apparent reduction in the grain size of mullite with 0.5 wt % zirconia with increasing temperature is attributed to the crystallization of tetragonal zirconia particles which effectively inhibited the exponential grain growth. A similar effect is also exhibited in the composite with 1.0 wt % zirconia. Monoclinic and tetragonal zirconia were obtained in the composite containing 7 wt % zirconia (Table I). It appears that only coarse zirconia particles ( $> 30$  nm) might be the main factor in the grain refinement of mullite. The inherent fine grains in the pure mullite and their persistence at high temperatures may be attributed to the microporous texture present which serves to suppress the various diffusion mechanisms essential for grain coarsening.

The apparent activation energies from the Arrhenius plot of Fig. 7 suggest that only mullites with 7 wt % zirconia or greater have lower activation energies than that of pure mullite. Because of the several mechanisms involved, no particular mechanism can be related to these qualitative activation energies; but, they do serve to indicate the strong temperature dependence and chemical control of grain growth. This observation is consistent with the results reported by McGee and Wirkus [16] where the presence of  $TiO_2$

Figure 3 (a) Plot of cell edge,  $a$ , against composition of mullite. The numbers indicate the amount of zirconia. (○)  $1250^\circ C$ , (●)  $1300^\circ C$ , (□)  $1300^\circ C$  (10 h). (b) Plot of cell volume,  $C_v$ , against cell edge,  $a$ , for mullite-zirconia gels treated at  $1300^\circ C$ . The numbers indicate the amount of zirconia in the composite. (—) [15], (---) present work, (— · —) [14]. (c) Variation of lattice parameters of mullite with  $ZrO_2$  content. (●)  $a$ , (■)  $b$ , (○)  $c$ .



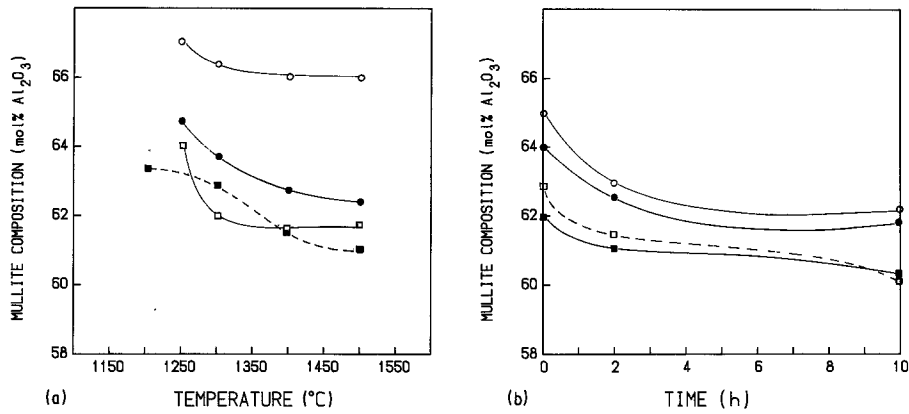


Figure 4 (a) Composition of mullite as a function of temperature. (■) Pure mullite; (○) 1 wt % ZrO<sub>2</sub>; (●) 5 wt % ZrO<sub>2</sub>; (□) 7 wt % ZrO<sub>2</sub>. (b) Composition of mullite as a function of time. (□) Pure mullite; (○) 0.5 wt % ZrO<sub>2</sub>; (●) 2 wt % ZrO<sub>2</sub>; (■) 7 wt % ZrO<sub>2</sub>.

retarded the grain growth of mullite and the reverse was true for the presence of Fe<sub>2</sub>O<sub>3</sub>.

The accuracy of grain size measurement by the X-ray line broadening technique is substantiated by the electron micrographs of composites as shown in Fig. 8. Grains of mullite with zirconia in solid solution have average size of  $> 1 \mu\text{m}$ . The composite with zirconia content of 5 wt % has mullite grain size of  $\approx \frac{1}{2} \mu\text{m}$  which approximates rather well with the calculated value. Evidently, the grain-growth controlling effect of zirconia is established. It is postulated that a zirconia-rich mullite solid solution forms in composites with contents of zirconia below the solubility limit and intragranular tetragonal zirconia particles crystallize out when the limit is surpassed. Intergranular zirconia particles (both tetragonal and monoclinic) are believed to crystallize only in composites with more than 5 wt % zirconia.

## 4. Discussion

### 4.1. Aspects of solid solution formation

Solid solutions are frequently met in binary metallic systems. A solid solution involves a solidification of an alloy with the formation of one kind of crystal in which both metals are present but cannot be detected microscopically. The incorporation of one metal into another can be realized either by substitution or as interstitials. The former is most frequently met, while the latter occurs only if the interstitial ions are small enough to be accommodated in the interstices of the parent metal. The major factors which allow extensive formation of a solid solution by substitutions of ions are (i) size factor, (ii) valency factor, (iii) chemical affinity and (iv) structure type.

The above factors reflect variations in the free energy of a crystal structure. The lowering of free energy by the random introduction of foreign atoms into the parent structure (due to higher entropy) results in a stable configuration of a solid solution being formed. When this occurs, there is usually a change in the cell size with composition in accordance with Vegard's law that lattice cell dimensions vary linearly with the concentration of solute added.

For oxides, particularly the ceramics, the major factors affecting the formation of a solid solution are the relative ionic sizes and valencies. Although difference in ionic sizes definitely preclude extensive solid solution formation, valence differences can frequently be made up by (a) exchange ions (e.g. hydroxyl ions) being absorbed on the crystal surface and (b) leaving an occasional atom site vacant, a phenomenon particularly common in spinels. In addition, oxide ceramics often display krypto-isomorphism, a phenomenon which prevails when the two crystal structures have similar sequence of atoms along any arbitrary lattice row. The surroundings of any atom are topologically identical in these two structures and only angles and distances are slightly different. Krypto-isomorphs, if they meet other requirements, can often form continuous series of solid solutions with one another via the entry of excess atoms of one type into sites that are vacant or into holes in the structure of the other.

### 4.2. Formation of solid solutions between zirconia and mullite

Mullite has been found to form solid solutions with Fe<sub>2</sub>O<sub>3</sub>, Cr<sub>2</sub>O<sub>3</sub> and TiO<sub>2</sub> mainly as impurities. The

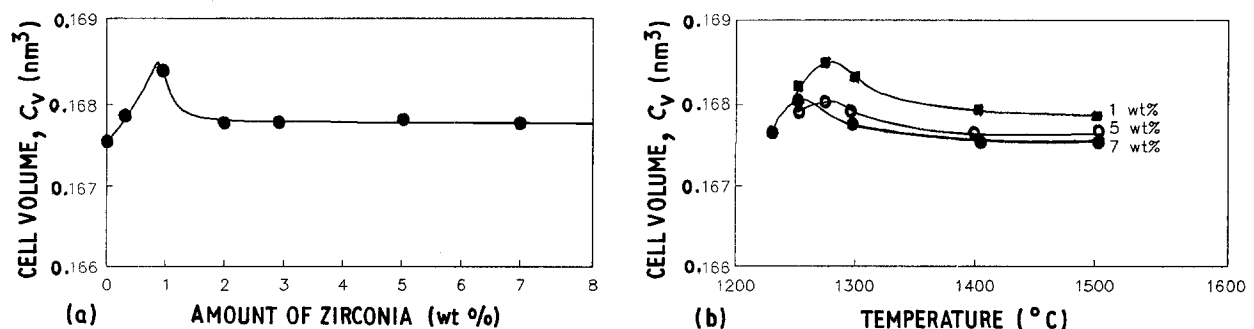


Figure 5 Variation of cell volume of mullite with (a) the amount of zirconia at 1300°C and (b) temperature (■) 1 wt % ZrO<sub>2</sub>; (○) 5 wt % ZrO<sub>2</sub>; (●) 7 wt % ZrO<sub>2</sub>.

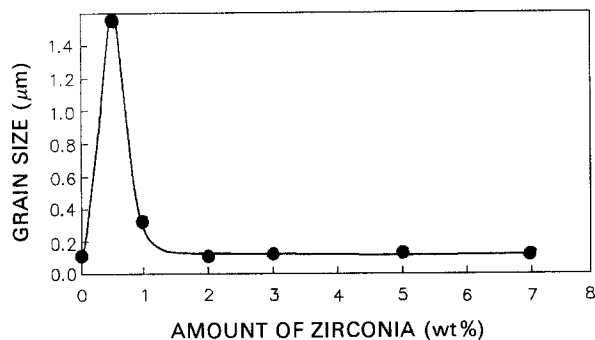


Figure 6 Variation of mullite grain size with the amount of  $ZrO_2$  added at  $1300^\circ C$ .

extent of solid solution of mullite with the various compounds are summarized in Table II. A perusal of the results serves to verify the ionic size factor as a limiting criterion for the formation of an extensive solid solution. Because the ionic radius of  $Zr^{4+}$  is  $0.072\text{ nm}$ , the extent of solid solution between zirconia and mullite is expected to be less than  $3.0\text{ wt}\%$  ( $\approx 9.7\text{ mol}\%$ ) at high temperatures.

The results enumerated in Fig. 5a suggest a maximum solid solution of about  $0.9\text{ wt}\%$  ( $3\text{ mol}\%$ ) zirconia in the matrix of mullite at  $1300^\circ C$ . This value is substantiated by the petrographic phase analyses (Table I) and is in accordance with the values obtained elsewhere [8–10].

Paulings ionic radii for  $Al^{3+}$ ,  $Si^{4+}$  and  $O^{2-}$  are  $0.051$ ,  $0.041$ ,  $0.072$  and  $0.0140\text{ nm}$ , respectively. Octahedral coordination is normally stable for cation-anion radius ratios of  $0.41$  to  $0.73$ ; and tetrahedral is normally stable for ratios between  $0.22$  and  $0.41$ . These ratios for aluminium, silicon and zirconium are  $0.37$ ,  $0.29$  and  $0.51$ , respectively. Therefore, zirconium ions would be expected to appear only in octahedral coordination. Considering the ratios of  $Si/Zr$  and  $Al/Zr$  with values of  $0.57$  and  $0.71$ , respectively, it is postulated that the solid solution of zirconia in mullite would involve the substitution of zirconium ions for aluminium ions. However, this mechanism predicts a higher value of solid solution with increasing temperatures because the diffusion-controlled ionic substitution can occur more readily at high temperatures. This assertion is in contradiction with the results

TABLE II Solid solutions of mullite with various compounds

Compounds	Extent of Solid solution (wt %)	Ionic radius (nm)	Temperature ( $^\circ C$ )
$Fe_2O_3$	7.6 [21]	0.064	1300
	10.0 [22]		1300
	8.0 [23]		1400
	12.0 [24]		1300
$Cr_2O_3$	9.0 [23]	0.062	1700
	9.0 [24]		1600
$TiO_2$	2.5 [23]	0.068	1700
	2.27 [25]		1700
	2.9 [26]		1600
	4.0 [27]		1700
$ZrO_2$	0.5 [8]	0.072	1350
	0.1 [10]		1600
	0.9 [12]		1300

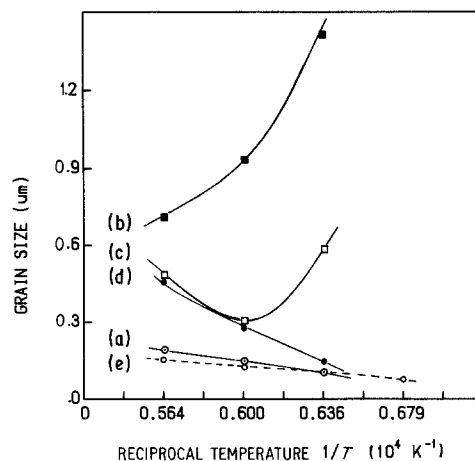


Figure 7 Arrhenius plot of mullite grain size against reciprocal temperature. (○) Pure mullite; (■)  $0.5\text{ wt}\%$   $ZrO_2$ ; (□)  $1\text{ wt}\%$   $ZrO_2$ ; (●)  $2\text{ wt}\%$   $ZrO_2$ ; (○)  $> 7\text{ wt}\%$   $ZrO_2$ .

obtained in this and other investigations. Results given in Table I and Fig. 5b clearly indicate that higher temperatures and longer heating times reduce the solid solubility of zirconia in mullite to well below  $0.9\text{ wt}\%$ . Similarly, Moya and Osendi [9] observed a metastable solid solution of zirconia ( $\approx 0.5\text{ wt}\%$ ) in mullite at  $1570^\circ C$ . This value was found to drop to  $\approx 0.1\text{ wt}\%$  at  $1600^\circ C$  by Pena and Aza [10]. Hence, the postulation that the substitution of  $Zr^{4+}$  for  $Al^{3+}$  as the most probable mechanism for the formation of solid solution between zirconia and mullite may only be true at high temperatures where the state of equilibrium in the system is readily reached, but it may be too simplistic to account for the much larger value of metastable solid solution at low temperatures where up to  $5\text{ wt}\%$  ( $\approx 15\text{ mol}\%$ ) zirconia may be incorporated into the structure of (2:1) mullite. A new model is obviously required for the latter.

The crystal structure of mullite consists of octahedral  $AlO_6$  chains, running parallel to the  $c$ -axis. The octahedral chains are cross-linked by tetrahedral  $(Al, Si)O_4$  double chains. The latter are distorted in such a way that some of the oxygen atoms of the common corners of two tetrahedra are missing; oxygen vacancies are therefore generated. There are various possible structural positions in the lattice of mullite which are suitable for entry of foreign cations to form a solid solution:  $AlO_6$ -octahedra,  $(Al, Si)O_4$  tetrahedra, random positions in the channels running parallel to the  $c$ -axis, interstices and structural voids produced by oxygen vacancies. It has been suggested that  $Fe^{3+}$ ,  $Ti^{4+}$  and  $Cr^{3+}$  substitute for  $Al^{3+}$  at octahedral positions.

A perusal of results obtained as depicted in Figs 1 to 5 serves to indicate that the mullite initially formed is alumina-rich, i.e. close to (2:1) composition, which gradually transforms to the equilibrium (3:2) composition at higher temperatures and longer periods of equilibrium heat treatment. The results also suggest that the (2:1) mullite has a low density and the structure is stricken with defects of various types while the (3:2) mullite has a higher density because of the presence of minimal crystal defects and a smaller cell volume. The fact that much more zirconia could be

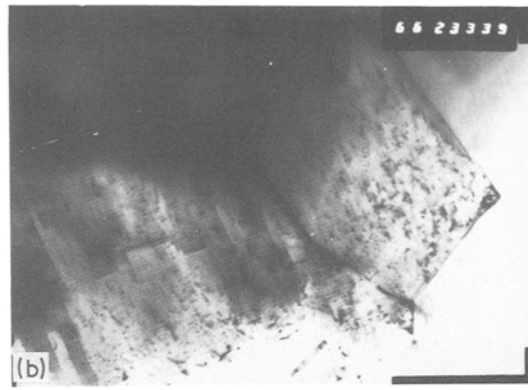
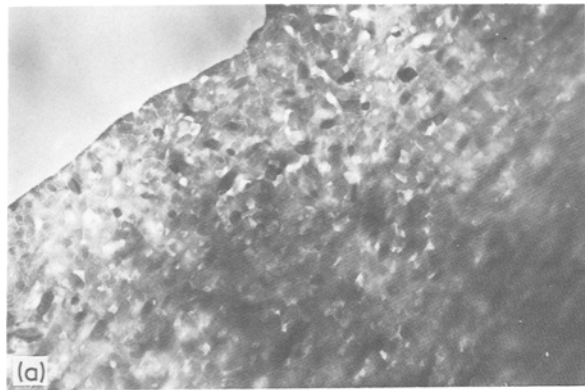


Figure 8 Electron micrographs of mullite-zirconia composites containing various amounts zirconia heat treated at 1300°C. (a) Pure mullite; (b) 0.5 wt % ZrO<sub>2</sub>; (c) 5 wt % ZrO<sub>2</sub>.

accommodated in the lattice of mullite at low temperatures ( $\leq 5$  wt %) may invite the hypothesis that in addition to the limited liberal substitution of Zr<sup>4+</sup> for Al<sup>3+</sup> as allowed by the valence and size criteria, the majority of zirconium ions are most probably “stuffed” at the interstices and/or vacancy domains of the (2:1) mullite lattice. The excess charge resulting from the incorporation of zirconium ions is probably compensated by substitution of silicon by aluminium atoms. The electrical neutrality may also be maintained via vacancy formation. At higher temperatures or longer heating times, a well crystallized mullite is formed with smaller cell dimensions. This transformation would result in the relatively large zirconium ions to be literally “squeezed” out of the lattice structure because of diminishing cell dimensions.

The variation of cell dimensions may be interpreted in terms of the type of crystal structure formed and the formation of solid solutions. Because of the comparatively large ionic radius, the zirconium ions are expected to go into the octahedral chains. The Al-O distance is close to 0.178 nm [17], and from the cell dimensions of the cubic lattice of zirconia, the Zr-O distance approximates 0.190 nm. Using these values, complete substitution of zirconium for aluminium in the octahedral chains should result in an increase of about 7% in the *c*-dimension. It follows that with the substitution of 5% Zr for aluminium in the octahedral columns should lead to around 0.35% increase in the *c*-dimension. However, the experimental results (Fig. 3c) for the mullites with 5 wt % ( $\approx 15$  mol %) ZrO<sub>2</sub> only indicate an increase in the *c*-dimension of around 0.035%! Hence, only a limited number of zirconium atoms could have substituted for aluminium atoms in the octahedral chains. The largest change in the cell dimension of this sample was that of

*a* which approximates to 0.10%. Because zirconium atoms are not expected to go into the tetrahedral positions, the large variation in the *a*-dimension could not have been due to substitution of zirconium atoms for aluminium atoms in the AlO<sub>4</sub> chains. It appears, therefore, that most of the zirconium atoms in solid solution may have, in fact, resided over the interstices and/or vacancy domains of the mullite lattice structure.

In pure mullites, the *c*-dimension should be nearly identical for there could be nothing but aluminium atoms in octahedral chains. The fact that the *c*-dimension changes linearly with temperature and composition suggests that some sort of reaction might have taken place. It is believed that the smaller cell dimensions and hence the diminishing cell volume of the mullite lattice at high temperatures are probably the results of: (i) strengthening of Al-O bonds in the octahedral chains and (Al, Si)-O bonds in the tetrahedral chains, and (ii) substitution of silicon for aluminium atoms in the tetrahedral chains, causing the bond lengths and hence the cell dimensions to diminish following the transformation of (2:1) to (3:2) mullites.

The mechanism of solid solution formation between (2:1) mullite and zirconia involves probably, in addition to the foregoing “stuffing” principle, the krypto-isomorphism of the two crystals. At low temperatures, both zirconia and (2:1) mullite have a similar crystal structure, i.e. tetragonal form. The similarity in the morphology of lattice atoms between the crystals would strongly enhance the interstitial (“stuffing”) solid solution of zirconia at low temperatures. At high temperatures, this phenomenon of krypto-isomorphism would be lost because of the formation of orthorhombic (3:2) mullite and either tetragonal or monoclinic zirconia. The well-crystallized mullite has minimal vacancy domains and smaller interstices because of a diminishing cell volume. Consequently, only a limited number of zirconium atoms can be stuffed into the well-compact mullite structure, resulting in the formation of a very limited solid solution. Moreover, the metastable zirconia particles would grow rapidly in size with increasing temperatures to hinder their stuffing into the mullite

structure. The oversize particles would be readily excluded as zirconia crystals.

The higher value of metastable solid solution observed at low temperatures may also arise from the local compositional variations, which prevail in submicrometre grains of the metastable mullite, by tolerating a higher concentration of zirconium atoms in the matrix. Both compositional equilibration and homogenization would be attained as the grains grow bigger. This would result in the lowering of entropy in the matrix and a smaller amount of zirconia would be tolerated. In summary, the complexity of the mechanisms involved in the formation of a metastable solid solution at low temperatures, is highlighted. No single mechanism may be the sole origin of this formation and it is the combination of a few mechanisms operating in concert which actually controls the formation of this elusive solid solution.

#### 4.3. Microstructural modifications in mullite–zirconia composites

Grain-growth inhibition is desirable for preventing abnormal grain growth during sintering, which allows pores to be swallowed to limit end-point densities and for limiting grain size to achieve higher strength. Theory that treats the inhibition of grain growth by inclusions has generally been based on refinements of Zener's [18] original concept, in which the inclusion residing at the grain boundary produces a dragging force due to the lower free energy of the junction/inclusion system when the inclusion resides at the junction. Ashby and Centamore [19] showed that the inclusion(s) can move with the junction if the inclusion exhibits sufficient self-diffusion.

Grain-size data (Figs 6 and 7) of mullite–zirconia composites indicate that exponential grain growth of mullite occurred when the zirconia inclusions remained completely in solid solution. Crystallization of tetragonal zirconia particles at temperatures below 1300°C appeared to be capable of arresting the abnormal grain growth. At higher temperatures, even the crystallized tetragonal zirconia particles could not stop the mullite grains from growing exponentially. Only for composites with zirconia content equal to or greater than 7 wt % was there any grain-growth inhibition from the inclusions. Apparently, below that critical amount, the distribution of zirconia particles is not sufficiently uniform to hinder the growth of all the mullite grains, resulting in formation of some exaggerated grains which tend to consume both fine neighbouring grains and zirconia inclusions. Above the critical amount of 7 wt % zirconia, in addition to the uniform distribution of intragranular and intergranular tetragonal zirconia particles, the presence of much coarser, intergranular monoclinic zirconia particles might exert a considerably larger dragging force to facilitate the inhibition of grain growth.

The abnormal grain growth of mullites with the composition of zirconia in the optimum range of solid solution may be attributed to the enhancement of bulk and grain-boundary diffusion processes which give rise to the acceleration of grain coarsening. The presence of zirconia in solid solution may serve to

indicate its potential application as a sintering aid for mullites. It follows, therefore, that crystallization of tetragonal and especially monoclinic zirconia particles in the matrix of mullite serve to depress the diffusional mechanisms and activation energy associated with grain coarsening, resulting in the refinement of mullite grains. The Arrhenius plot of Fig. 7 suggests that a relation exists between grain size and activation energy.

The grain-growth controlling effect of zirconia has also been observed by Prochazka *et al.* [3]. They found that in addition to grain refinement, addition of zirconia (10 to 25 vol %) also promoted densification of mullite and a microstructure relatively free of glassy phase was obtained. The presence of coarse monoclinic zirconia particles which were dispersed intergranularly may suggest that the origin of grain-growth inhibition is probably due to the phenomenon proposed by Zener [18]. A contradictory observation was reported by De Portu and Henney [20] where grain coarsening was obtained in the microstructures of mullite with 10 to 17 vol % zirconia. However, they did observe substantial strengthening and toughening in the composites which are in good agreement with those of Prochazka *et al.* [3].

#### 5. Conclusions

Composites of mullite with zirconia contents up to 20 wt % zirconia were prepared by the gel method. The presence of zirconia appeared to enhance the formation and sintering of (3:2) mullite. The formation of a metastable solid solution between zirconia and mullite was established. At 1300°C, the solid solubility of zirconia in mullite was  $\approx 0.9$  wt %. This value was observed to decrease with increasing temperatures and heating times and vice versa. The maximum metastable solubility was about 5 wt % zirconia and it occurred most likely in the spinel or the metastable aluminous mullite.

The mechanism of solid solution formation in the equilibrium (3:2) mullite involved probably the substitution of zirconium for aluminium atoms in the octahedra chains. This value is most probably less than 0.1 wt % zirconia. The origins of metastable solid solution between zirconia and (2:1) mullite were very complex but they are believed to involve predominantly the "stuffing" of zirconium atoms at the interstices and vacancy domains of the defects stricken (2:1) mullite lattice structure. "De-stuffing" of zirconium atoms from these locations occurred at high temperatures when a smaller cell volume, more compact and well-crystallized (3:2) mullite was formed.

The presence of zirconia in solid solution with mullite appeared to cause abnormal coarsening of mullite grains. Grain refinement of mullite could only be achieved by the presence of at least 7 wt % zirconia. Coarse and intergranularly dispersed monoclinic zirconia particles were most effective as grain growth inhibitors.

#### Acknowledgement

We thank Monash University for providing a research scholarship to one of us (I.M.L.).

## References

1. N. CLAUSSEN and J. JAHN, *J. Amer. Ceram. Soc.* **63** (1980) 228.
2. N. CLAUSSEN, *ibid.* **59** (1976) 49.
3. S. PROCHAZKA, J. S. WALLACE and N. CLAUSSEN, *ibid.* **66** (1983) C125.
4. C. A. SORRELL and C. C. SORRELL, *ibid.* **60** (1977) 495.
5. G. FAGHERAZZI and S. ENZO, *J. Mater. Sci.* **15** (1980) 2693.
6. A. MAKISHIMA, H. OOSHASHI, M. WAKAKUWA, T. SHIMOHIRA and K. KOTANI, *J. Non-Cryst. Solids* **42** (1980) 545.
7. R. McPHERSON, to be published.
8. J. S. MOYA and M. I. OSENDI, *J. Mater. Sci. Lett.* **2** (1983) 599.
9. *Idem*, *ibid.* **19** (1984) 2909.
10. P. PENA and S. DE AZA, *Sci. Ceram.* **9** (1977) 247.
11. G. C. WHITAKER, *Adv. Chem. Ser.* **23** (1957) 184.
12. I. M. LOW, PhD thesis, Monash University (1986).
13. I. M. LOW and R. McPHERSON, Proceedings of the 11th Australian Ceramic Society Conference (Australian Ceramic Society, 1984) p. 471.
14. W. E. CAMERON, *Amer. Mineral.* **62** (1977) 747.
15. H. SCHNEIDER and K. WOHLBEN, *Ceram. Int.* **7** (1981) 130.
16. T. D. MCGEE and C. D. WIRKUS, *Bull. Amer. Ceram. Soc.* **51** (1972) 577.
17. J. V. SMITH, *Acta Crystallogr.* **7** (1954) 479.
18. C. ZENER, *Trans. Met. Soc. AIME* **175** (1949) 15.
19. M. F. ASHBY and R. M. A. CENTAMORE, *Acta Metall.* **16** (1968) 1081.
20. G. DE PORTU and J. W. HENNY, *Br. Ceram. Soc.* **83** (1984) 69.
21. N. E. BROWNELL, *J. Amer. Ceram. Soc.* **41** (1985) 226.
22. A. MUAN, *ibid.* **40** (1957) 121.
23. G. GELSDORF, H. MULLER-HESSE, H. E. SCHWIETE and H. WESTMARK, *Ceram. Abstr. Sept.* (1959) 236e.
24. M. K. MURTHY and F. A. HUMMEL, *J. Amer. Ceram. Soc.* **43** (1960) 267.
25. S. V. AGRELL and J. V. SMITH, *ibid.* **43** (1960) 69.
26. C. BAUDIN, M. I. OSENDI and J. S. MOYA, *J. Mater. Sci. Lett.* **2** (1983) 185.
27. C. R. GREEN and J. WHITE, *Trans. J. Br. Ceram. Soc.* **43** (1974) 73.

*Received 11 December 1987  
and accepted 13 May 1988*